

MULTI-SCALE FATIGUE OF AS-CAST LIGHTWEIGHT STRUCTURAL METALS

Ken Gall¹, Mark Horstemeyer², David L. McDowell³, Jinghong Fan³, and Nancy Yang²

¹Department of Mechanical Engineering, University of Colorado, Boulder, CO, 80309 USA

²Materials & Engineering Sciences Center, Sandia National Laboratories,
Livermore, CA 94550 USA

³GWV School of Mechanical Engineering, Georgia Institute of Technology,
Atlanta, GA 30332 USA

ABSTRACT

We present an overview of a multiscale modeling approach whereby we examine basic mechanisms of fatigue deformation at length scales ranging from nanometers to millimeters, as necessary to treat hierarchical heterogeneous microstructural features in castings. A coordinated numerical and experimental effort is outlined that employs atomistic simulations, finite element modeling, electron microscopy, and mechanical testing. Atomistic and realistic micro-mechanical simulations of representative microstructural features are used to elucidate the role of different microstructural constituents such as Si particles, pores, and oxides on fatigue crack nucleation and growth. Ultimately, we demonstrate that fatigue life prediction methodologies can be developed that explicitly incorporate features of the cast microstructures.

KEYWORDS

Cast Al-Si, Defects, SEM, modeling, finite element, atomistic, fatigue life predictions.

INTRODUCTION

Current fuel consumption and cost demands in the automotive industry are facilitating the widespread use of lightweight cast materials for structural components. Although cast components have always enjoyed certain economic advantages compared to wrought materials, they are usually over-designed due to processing related variability within and between components. Most existing fatigue life prediction approaches have been primarily developed in the context of wrought materials, and they do not provide clear paths for optimal casting design. The present paper overviews a methodology developed to understand and predict the fatigue of cast materials over multiple length scales. The techniques are only summarized here, and interested readers should consult the papers referenced within for details. A similar approach was also employed to understand and predict the monotonic failure of cast Al-Si alloys [1].

FATIGUE MECHANISMS

Extensive Scanning Electron Microscope (SEM) observations of the fracture surfaces of fatigued cast A356 aluminum samples has been performed to characterize the critical mechanisms of fatigue crack nucleation and growth [2, 3]. Following Figure 1, fatigue cracks

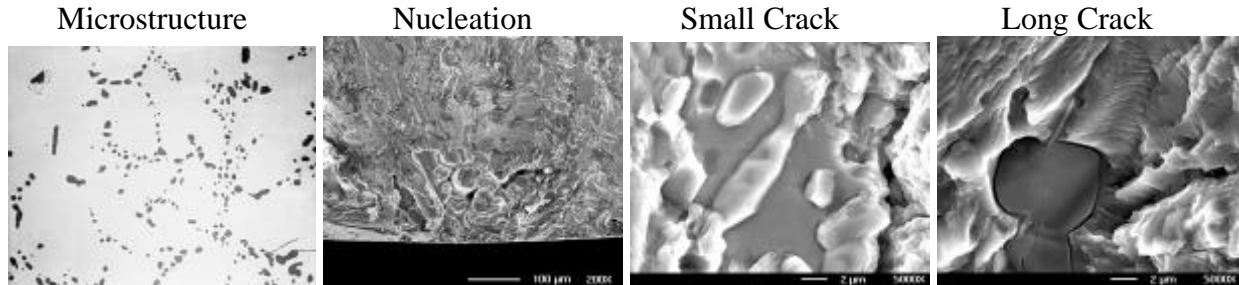


Figure 1: SEM images of the microstructure and progression of fatigue damage in cast Al-Si subjected to high cyclic fatigue loading conditions [2,3].

are found to preferentially nucleate at inhomogeneities such as voids or trapped oxide inclusions. Subsequent to nucleation, the cracks typically progress as microstructurally small cracks whereby the Si particles act as barriers and the cracks can only pass them by debonding (Figure 1). If the nucleation site is large enough, the crack may bypass the microstructurally short stage. On the other hand, longer cracks propagate through the Si particle laden microstructure via the fracture of large irregular particles (Figure 1). From SEM observations, it is clear that the Si particles can act as barriers or weak links to fatigue crack propagation, depending on the crack tip driving force [2, 3]. To develop a physically-based model, one must account for the critical roles of the Si particles, voids, and other inhomogeneties on fatigue crack nucleation and growth.

ATOMISTIC AND MICRO-MECHANICAL MODELING

Atomic level simulations [4] were used to ascertain the local strength of the Al-Si interface in the as-cast material since this quantity was not easily measured experimentally. Figure 2 is an image from a Modified Embedded Atom Method (MEAM) simulation showing the debonding of a composite aluminum and silicon block attached at a $[100]_{Al}||[100]_{Si}$

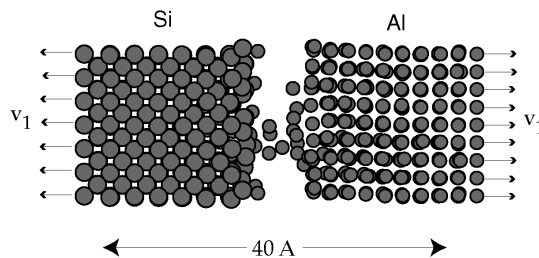


Figure 2: MEAM simulation on the debonding of an Al-Si interface [4].

interface, and subjected to far field velocities. The results of [4] demonstrated that the interface debonds at about 2/3 the stress before the bulk Al material fails. In the absence of vacancies, dislocations, impurities, and mechanical defects, the nucleation of interfacial fracture occurs at the atomic positions where the local displacement of interface atoms creates a rippled structure. Moreover, the debonding of the interface was found to behave nearly identical to continuum-based traction separation models. In terms of higher scale modeling, the atomic level

simulations provided knowledge on the relative strength of the interface compared to the bulk materials, and support for using traction-separation laws in micro-mechanical finite element simulations. Micro-mechanical finite element simulations were conducted to study the local plastic shear strains near voids and inclusions [5] and stress distributions near Si particle clusters [6]. Figure 3 is a representative example demonstrating local cyclic plasticity near a debonded inclusion [5]. The contour plot on the left in Figure 3 shows the development of local plastic

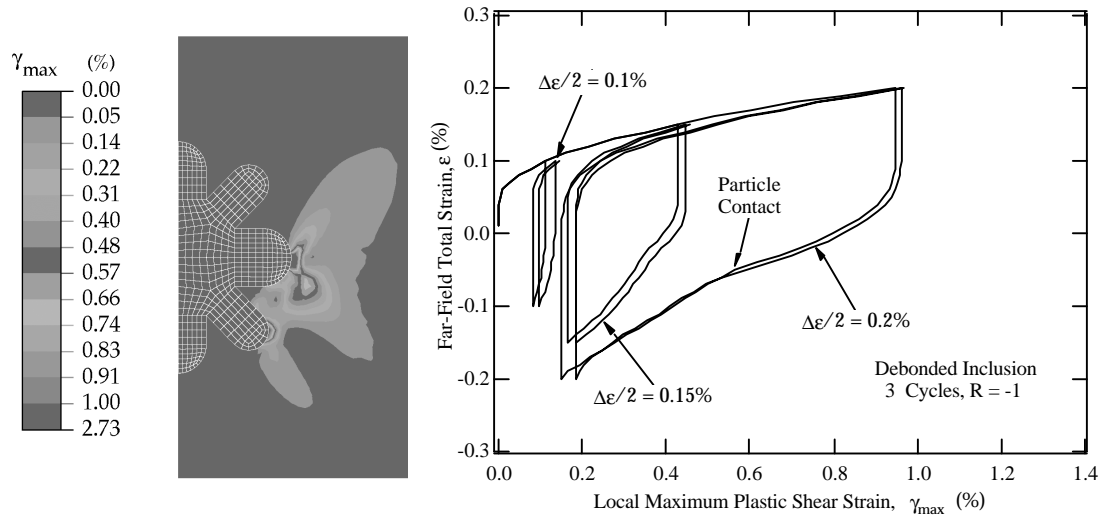


Figure 3: Local plastic shear strains near a debonded inclusion [5].

shear strains on the order of a few percent near a debonded star shaped inclusion under an applied far-field strain of 0.2 %. The plot on the right in Figure 3 shows the relationship between the far-field strain and the local maximum plastic shear strain, γ_{\max} , averaged over a finite area [5]. Although the far-field strain is fully reversed ($R = -1$), the local plastic shear strain does not reverse itself. Furthermore, the local plastic shear strain range is as high as a 1 % even when the far-field strain range is nominally elastic (0.2 %). The results in [5] quantified the plastic strain levels as a function of inhomogeneity type, shape, and size, and external factors such as R-ratio and applied far-field strain range. Debonded inclusions and voids were predicted to be the critical inhomogeneities for fatigue crack formation. Furthermore, for voids and debonded inclusions, shape has a negligible effect on fatigue crack formation compared to other significant effects such as inhomogeneity size and R ratio. Increasing the size of an inclusion by a factor of four increases $\Delta\gamma_{\max}$ by about a factor of two. At low R ratios (-1) equivalent sized voids and debonded inclusions have comparable $\Delta\gamma_{\max}$ values. At higher R ratios (0, 0.5) debonded inclusions have $\Delta\gamma_{\max}$ values twice that of voids. Such results are critical for developing a mechanism and microstructure based fatigue crack nucleation model, as discussed later.

We also employed micro-mechanical finite element simulations to model the advancement of microstructurally small cracks in a Si particle laden microstructure [7]. The cracks were simulated to grow through the Al-rich matrix and through the silicon particles by successive particle-matrix interface debonding, commensurate with SEM observations. Figure 4 is an example result showing the fluctuation in the crack tip opening displacement as the crack approaches and grows around Si particles. The results show that as the crack approaches a particle, the maximum plastic shear strain range at the crack tip element decreases. However, as the crack impinges directly on the particle, the plastic shear strain range rapidly increases. The increase in the plastic shear strain range has been interpreted in terms of geometrically necessary

dislocations. The effects of initial crack length, applied strain amplitude, and crack closure on crack tip behavior show very strong effects of particles on the growth behavior of microstructurally small cracks. Although the crack opening displacement with a long initial crack length is much greater than a short one, once both cracks have engaged 2-3 silicon particles their difference is reduced and they follow a common retardation pattern. As the dendrite cell spacing increases, the crack closure period decreases. In the presence of particles, to a good approximation the crack is open only under tensile load.

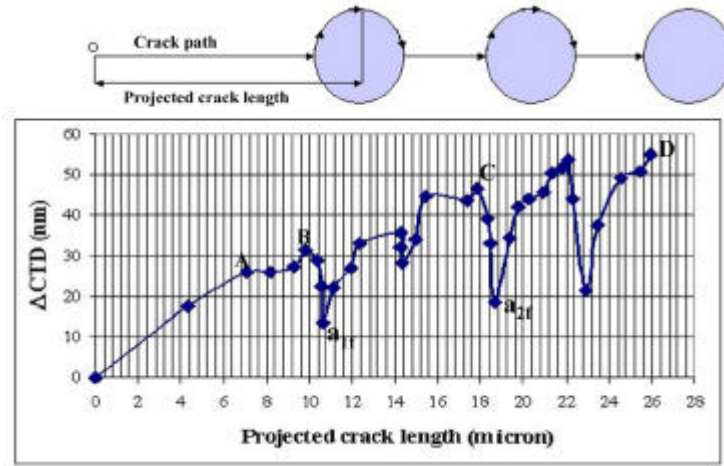


Figure 4: Finite element model of fatigue crack growth through a field of Si particles [7].

FATIGUE MODEL

Based on the foregoing computational results, along with experimental motivation from this study and other literature, a fatigue model was developed that is sensitive to the scale of initial inclusions and the dendrite cell size (DCS), e.g., Si particles and no significant pores or oxides, no large pores or oxides (length scale of $< 3DCS$), large pores within the bulk, large pores near the surface and large folded oxides. The fatigue life (for crack nucleation and growth up to about 1 mm, at which point the crack has transitioned to long crack status governed by ΔK_{eff} (LEFM), is governed by a set of relations that describes formation of cracks at micronotches such as gas pores or Si particles, followed by growth in the microstructurally sensitive regime characterized by a relatively small crack tip cyclic plastic zone and damage process zone compared to the mean Si particle size and spacing. The total fatigue lifetime is given by:

$$N_T = N_{inc} + N_{MSC} + N_{PSC} + N_{LC} = N_{inc} + N_{MSC/PSC} + N_{LC} \quad (1)$$

where N_{inc} is the number of cycles to incubation (nucleation plus small crack growth through the notch root influence) of a micronotch root scale crack with initial length, a_i , on the order of $1/2$ the maximum Si particle diameter, \hat{D}_{part} , or pore size, \hat{D}_p . Here, N_{MSC} is the number of cycles required for propagation of a microstructurally small crack (MSC) with length $a_i < a < k DCS$, where k is a non-dimensional factor that is typically in the range of 3-5. Further, N_{PSC} is the number of cycles required for propagation of a physically small crack (PSC) during the transition from microstructurally small crack status to that of a dominant, long crack which then propagates according to LEFM with an associated number of cycles N_{LC} . Since the DCS is typically on the order of 30 to 100 μm , depending upon the solidification rate, the PSC regime may conservatively extend up to 300-800 μm .

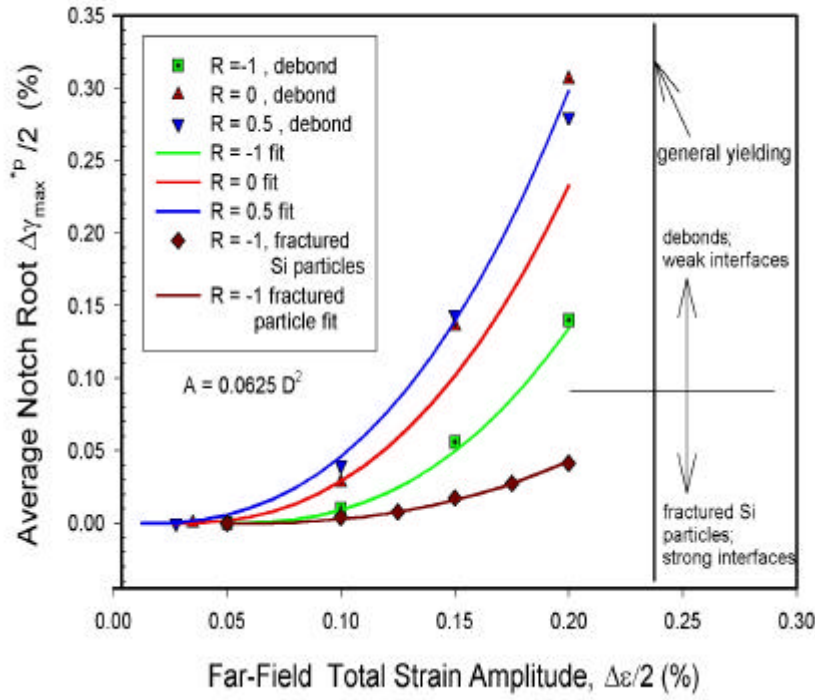


Figure 5: Relation between average notch root maximum plastic shear strain amplitude and applied total strain amplitude for micronotches (debonded or fractured Si particles or pores).

Using finite-element based transfer functions between remote applied strain and micronotch root strain, as shown in Figure 5, a local Coffin-Manson law is applied to determine the number of cycles required to form a crack and grow it outside the domain of influence of the notch root, N_{inc} . Then, using the MSC/PSC growth law

$$\left(\frac{da}{dN}\right)_{MSC/PSC} = G(\Delta CTD - \Delta CTD_{th}), \quad (2)$$

$$\Delta CTD = f(\bar{\varphi})C_{II} \left(\frac{DCS}{DCS_0}\right) \left[\frac{U\Delta\hat{\sigma}}{S_u}\right]^n + C_I \left(\frac{DCS}{DCS_0}\right) (\Delta\gamma_{max}^p / 2 |_{macro})^2$$

the MSC/PSC component of lifetime is computed, where $\bar{\varphi}$ is the average porosity, $U\Delta\hat{\sigma}$ is an effective normal stress range, and S_u is ultimate strength. DCS and DCS_0 are the current and reference dendrite cell size and $\Delta\gamma_{max}^p$ is the maximum plastic shear strain range over all possible shear planes. The second term governs fully plastic growth of small cracks. It is found that the HCF-LCF transition occurs at the point of percolation of cyclic microplasticity through the interdendritic eutectic regions, and nucleation lifetime is negligible above this effective strain amplitude (0.23% at $R = -1$). The transition to long crack LEFM-governed behavior is defined by the point where the crack growth rate in Equation (2) crosses over the da/dN data based on long crack ΔK_{eff} . Effects of coalescence of multiple small cracks that nucleate at various inclusions (Si particles and pores) in the microstructure are important to address in the LCF regime and result in a crossover of fatigue resistance; low porosity is essential to superior HCF resistance, whilst large, widely spaced pores actually assist the LCF resistance. The scatter in fatigue data for cast A356-T6 alloy can essentially be fully

described by the typical range of microstructure inclusions that are present in laboratory specimens (see Figure 6 below).

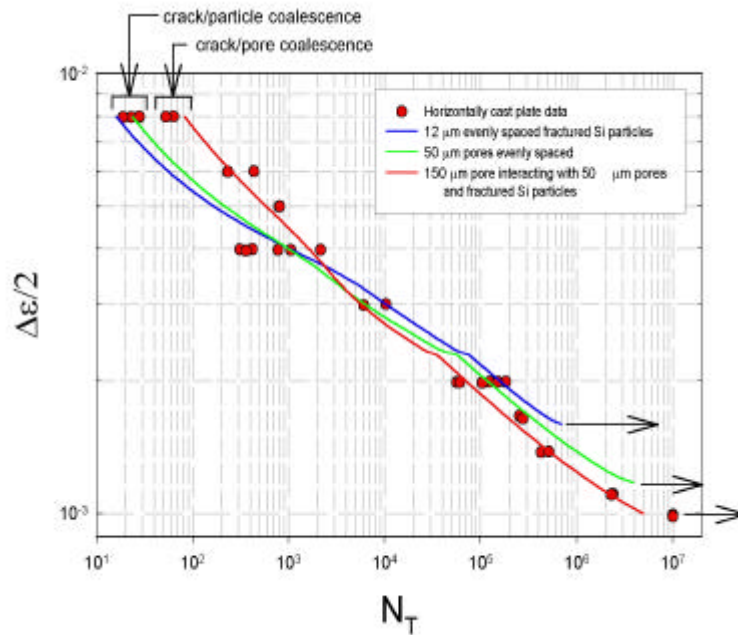


Figure 6: Variation in completely reversed, uniaxial strain-life behavior as a function of maximum inclusion size for horizontally cast plate, including LCF coalescence effects.

ACKNOWLEDGMENTS

This work has been sponsored by the U.S. Department of Energy, Sandia National Laboratories under contract DE-AC04-94AL85000. This work was performed under the leadership of Dick Osborne and Don Penrod for the USCAR Lightweight Metals Group. We would like to thank Gerry Shulke for providing the material and Westmoreland Mechanical Testing and Research for conducting the fatigue tests.

REFERENCES

- [1] Gall, K. and Horstemeyer, M. F. (2000) *J. Eng. Mat. Tech.*, 122, 355.
- [2] Gall, K., Yang, N., Horstemeyer, M. F., McDowell, D. L. and Fan, J. (1999) *Metall. Trans.*, 30A, 3079.
- [3] Gall, K., Yang, N., Horstemeyer, M. F., McDowell, D. L. and Fan, J. (2000) *Fat. Frac. Eng. Mat. Struc*, 23, 159.
- [4] Gall, K., Horstemeyer, M. F., Baskes, M. I., and Van Schilfgaarde, M. (2000) *J. Mech. Phys. Solids*, 48, 2183.
- [5] Gall, K., Horstemeyer, M. F., McDowell, D. L., and Fan, J (2001) In Press *Int. J. Frac.*
- [6] Gall, K., Horstemeyer, M. F., McDowell, D. L., and Fan, J (2000) *Mech. Mat.* 32, 277.
- [7] Fan, J., McDowell, D. L., Horstemeyer, D. L., Gall, K., (2001) Submitted *Eng. Frac. Mech.*